Desalination and Water Treatment
www.deswater.com

doi: 10.1080/19443994.2014.880381

52 (2014) 4029–4039
June

Taylor & Francis
Taylor & Francis Group

Modelling the NOM uptake by anion exchange resins in drinking water plants

Madlen Pürschel[a,*], Volker Ender[a], Eckhard Worch[b]

[a]*Faculty of Mathematics/Natural Sciences, University of Applied Sciences Zittau/Görlitz, Theodor-Körner-Allee 16, 02763 Zittau, Germany*
Tel. +049 3583 611707; Fax: +049 3583 611740; email: m.puerschel@hszg.de
[b]*Faculty of Environmental Science, Dresden University of Technology, Helmholtzstraße 10, 01069 Dresden, Germany*

Received 14 November 2013; Accepted 1 January 2014

ABSTRACT

In drinking water treatment plants, the removal of natural organic matter (NOM) is an essential aim to improve the final water quality and to reduce the formation of disinfection by-products. The objective of the present study was to compare the performance of different macroporous anion exchange resins (AERs) with regard to their NOM removal under drinking waters conditions. NOM removal at neutral pH was assessed by measuring the decrease of the dissolved organic carbon concentration in equilibrium experiments. Further, the fictive component approach (adsorption analysis) was applied to describe the competitive adsorption equilibria of the complex NOM system. Due to their relevance for fixed-bed filter design, breakthrough curves (BTCs) were measured and modelled by the homogeneous surface diffusion model with the linear driving force approach for surface diffusion combined with the ideal adsorbed solution theory for competitive adsorption. These model approaches, well known from activated carbon adsorption, were used in the present study to describe NOM adsorption onto AERs. The required mass transfer coefficients were obtained by empirical correlations. The applicability of the BTC model was verified with the experimental data of NOM uptake onto one selected AER.

Keywords: Natural organic matter; Drinking water; Anion exchange; Adsorption; Breakthrough curve; LDF model

---

1. Introduction

Natural organic matter (NOM) occurs in all raw water sources used for drinking water production. NOM is a complex mixture of organic materials such as biopolymers, humic substances, building blocks, low molecular weight (LMW) neutrals and LMW acids. The removal of NOM is one of the main aims in drinking water treatment, since it can cause (i) colour, taste and odour problems, (ii) formation of carcinogenic halogenated disinfection by-products (DBPs) after disinfection with chlorine and (iii) bacterial re-growth in the water distribution system (e.g. [1–3]).

Treatment processes used to remove NOM include enhanced coagulation and nanofiltration as well as adsorption onto activated carbon, anion exchangers, activated alumina and ferric hydroxide (e.g. [2,4–8]).

---

[*] Corresponding author.

Results from previous study indicate that anion exchange treatment is a very effective method for NOM removal from raw drinking water [9]. It was found that anion exchange resins (AERs) have the potential to adsorb more hydrophilic, charged NOM components which are not strongly removed by conventional techniques like enhanced coagulation [4]. Thus, if AERs are used in combination with conventional methods, it can offer another opportunity to reduce DBP formation by removing a broader variety of precursors [10].

Hence, the purpose of this study was to evaluate NOM uptake (measured as dissolved organic carbon; DOC) of different macroporous AERs at neutral pH conditions, which are typical for drinking water treatment. The AERs selected for the study differ especially in their functional groups (tertiary vs. quaternary amines) and matrix material (polystyrene vs. polyacrylic resins). The use of different AERs provides an option to identify possible interactions between NOM components and the AERs as well as the mechanism which determine the removal efficiency. This study includes the estimation of equilibrium and kinetic parameters of NOM adsorption and subsequently the prediction of breakthrough curves (BTCs). For BTC modelling, the fictive component approach (adsorption analysis) by Johannsen and Worch [11] was applied to describe the competitive adsorption equilibria of the complex NOM system. Further, the homogeneous surface diffusion model with the linear driving force (LDF) approach for surface diffusion [12,13] combined with the ideal adsorbed solution theory (IAST) for competitive adsorption were used to predict NOM uptake in fixed-bed AER columns at neutral pH. The applicability of the BTC model, originally developed for activated carbon adsorption, to describe the adsorption onto AER was verified by a fixed-bed filter experiment, where the NOM uptake onto one selected AER was measured.

2. Theory

In the present work, the LDF model, the IAST and the adsorption analysis were applied to evaluate NOM uptake performance of different AERs at neutral pH.

2.1. LDF model

The LDF model can be used to describe the adsorption processes in fixed-bed adsorbers. In this model, the mass balance equation can be written as follows (Eq. (1)):

$$v_F \frac{\partial c}{\partial z} + \varepsilon_B \frac{\partial c}{\partial t} + \rho_B \frac{\partial \bar{q}}{\partial t} = 0 \tag{1}$$

where v_F is the linear filter velocity (m/s), c is the concentration in the fluid phase (mg/L), z is the vertical travel distance within the adsorber (m), ε_B is the bed porosity (−), t is the time (s), ρ_B is the bed density (g/L) and $\bar{q}$ is the mean adsorbent loading of the solid phase (mg/g).

The adsorption kinetics is described by simplified mass transport equations based on the LDF approach proposed by Glueckauf [12]. The rate of film diffusion is given by Eq. (2) and the intraparticle (solid) diffusion, which includes pore and surface diffusion, is expressed in Eq. (3):

$$\frac{\mathrm{d}\bar{q}}{\mathrm{d}t} = \frac{k_F a_{VR}}{\rho_B}(c - c_s) \tag{2}$$

$$\frac{\mathrm{d}\bar{q}}{\mathrm{d}t} = k_S^*(q_s - \bar{q}) = \frac{k_S a_{VR}}{1 - \varepsilon_B}(q_s - \bar{q}) \tag{3}$$

where $k_F a_{VR}$ is the volumetric film mass transfer coefficient (s^{-1}), c_s is the concentration at the outer solid particle surface (mg/L), k_S^* is the intraparticle mass transfer coefficient (s^{-1}), which can be further separated into a mass transfer coefficient k_S (m/s) and a volume-related surface area a_{VR} (m^{-1}) like shown in Eq. (3) and q_s is the adsorbent loading at the outer particle surface (mg/g).

In the case of single solute adsorption, the Freundlich isotherm is applied to link concentration and loading at the outer particle surface by following Eq. (4):

$$q_s = K_F (c_s)^n \tag{4}$$

where K_F ((mg/g)/(mg/L)^n) and n (−) are the parameters of the Freundlich isotherm.

For application of the LDF model, Eqs. (1)–(4) are written in dimensionless form and are solved by numerical calculations (finite difference method) [13].

In the case of multi-solute adsorption, the Freundlich isotherm has to be substituted by a competitive adsorption model.

2.2. IAST

The IAST is widely accepted as standard method for modelling the competitive adsorption. It allows predicting competitive adsorption equilibria on the basis of single-solute adsorption data. If the single-solute equilibrium data of the mixture components are described by the Freundlich isotherm, the following set of Eqs. (5)–(7) can be derived from the IAST [13]:

$$\sum_{i=1}^{N} z_i = \sum_{i=1}^{N} \frac{c_i}{\left(\frac{\varphi \cdot n_i}{K_{F,i}}\right)^{1/n_i}} = 1 \tag{5}$$

$$q_T = \left[\sum_{i=1}^{N} \frac{z_i}{\varphi \cdot n_i}\right]^{-1} \tag{6}$$

$$q_i = z_i \cdot q_T \tag{7}$$

where z_i is the adsorbed phase mol fraction (−), φ is the spreading pressure term (−) and q_T is the total amount adsorbed (mg/g).

The IAST can be integrated into fixed-bed and batch adsorber models. The use of the IAST in BTC modelling was described, for instance by Worch [14,15] for the LDF model. For applying the IAST in a batch adsorber system, the basic Eqs. (5)–(7) have to be combined with a material balance for each component [13]. The material balance for component i is given by Eq. (8):

$$q_i = \frac{V_L}{m_A}(c_{0,i} - c_i) = \frac{V_L}{V_R \cdot \rho_B}(c_{0,i} - c_i) \tag{8}$$

where V_L is the volume of the liquid phase (L), m_A is the adsorbent mass (g), $c_{0,i}$ is the initial concentration (mg/L) and V_R is the reactor volume (L).

2.3. Adsorption analysis

BTC modelling for multi-solute systems requires the knowledge of the concentrations and isotherm parameters of all components. However, NOM is not a defined mixture. Therefore, the concentrations and the isotherm parameters of the different NOM fractions cannot be directly derived from DOC isotherm measurement. Applying the liquid chromatography—organic carbon detection (LC–OCD) analysis for each equilibrium experiment could be an option. Another, less expensive, method, which is used in the present work, is to apply a fictive (or hypothetical) component approach, the so-called adsorption analysis, after Sontheimer et al. [16] and Johannsen and Worch [11]. The principle of adsorption analysis consists in defining NOM fractions (mostly 3–5) with different adsorption performances characterized by individual Freundlich isotherm parameters (K_F and n). For simplification, n is normally held constant and only different K_F values are used to characterize the graduation of the adsorption strength. Further, a search routine based on the IAST is used to find that concentration distribution of the NOM fractions allows the best fitting of the experimental data of the DOC isotherm. As a result, the NOM is formally transformed to a “known” system for which the IAST can be applied in further fixed-bed or batch adsorber modelling.

2.4. Parameter estimation

To determine equilibrium data, the bottle-point (batch) method can be applied. The time required to reach equilibrium is typically between some hours and some weeks and has to be ascertained in preliminary kinetic studies. After the equilibrium is established, the adsorbed mass can be calculated using the material balance equation for batch adsorption processes (Eq. (8)).

The film and intraparticle mass transfer coefficients, required for BTC modelling, can be predicted by empirical correlations.

The volumetric film diffusion mass transfer coefficient, $k_F a_{VR}$ (s^{-1}) can be obtained from the dimensionless Reynolds (Re) and Schmidt (Sc) numbers by empirical correlations. Here, the correlation after Wilson and Geankoplis [17] was used (Eq. (9)). First, the dimensionless Sherwood number (Sh) is calculated by using Eqs. (9)–(11) and subsequently the film mass transfer, k_F (m/s) is found from the definition of Sh by Eq. (12) as follows:

$$\mathrm{Sh} = 1.09 \cdot \varepsilon_B^{-2/3} \cdot \mathrm{Re}^{1/3} \cdot \mathrm{Sc}^{1/3} \quad (\text{for } 0.0016 < \varepsilon_B \mathrm{Re} < 55 \text{ and } 950 < \mathrm{Sc} < 70{,}000) \tag{9}$$

The dimensionless numbers are defined as:

$$\mathrm{Re} = \frac{v_F \cdot d_P}{\varepsilon_B \cdot \nu} \tag{10}$$

$$\mathrm{Sc} = \frac{\nu}{D_L} \tag{11}$$

$$\mathrm{Sh} = \frac{k_F \cdot d_P}{D_L} \tag{12}$$

where d_P is the particle diameter (m), D_L is the liquid phase diffusion coefficient (m^2/s) and ν is the kinematic viscosity (m^2/s).

The required liquid phase diffusion coefficient D_L (m^2/s) is either known from the literature or can be obtained by the empirical correlation given by Worch [18] as follows (Eq. (13)):

$$D_L = \frac{3.595 \cdot 10^{-14} \cdot T}{\eta \cdot M^{0.53}} \tag{13}$$

where T is the temperature (K), η is the dynamic viscosity (Pa•s) and M is the molecular mass of the solute (g/mol).

The intraparticle mass transfer coefficient k_S^* (s^{-1}) can be predicted by an empirical correlation after Hess [19] using Eq. (14):

$$k_S^* = a + b\frac{c_{0(a)}}{r_P^2} \tag{14}$$

where $a = 3 \times 10^{-6}\,s^{-1}$ and $b = 3.215 \times 10^{-14}$ (m L)/(mg s) are empirical parameters, $c_{0(a)}$ is the total concentration of all adsorbable NOM fractions expressed as DOC (mg/L) and r_P is the particle radius (m).

3. Materials and methods

3.1. Anionic exchange resins

Four fresh macroporous AERs were used to study the NOM uptake from pre-treated water at neutral pH. The AERs were selected in order to cover a broad range in matrix material and functional groups (Table 1). AERs were applied in their hydroxide form. Resin characteristics were obtained from product data sheets of the manufacturers. The total volume (anion exchange) capacity (TVC in mol eq/L) of an AER, which is the sum of functional groups present on the resin material per volume, was calculated from the experimental sulphate BTC (up to $c/c_0 = 1$) by application of the integral mass balance equation for real BTCs. Sulphate BTCs were obtained from fixed-bed studies with 0.01 M Na_2SO_4 from KMF. The solution was prepared with Millipore water (conductivity < 1 μS/cm, pH = 5.8 and total organic carbon (TOC) < 50 μg/L) obtained from a Millipore ultrapure water system (Elix/Milli-Q Academics). The effluents were analysed by titration measurements with 0.02 M HCl as titration solution and bromothymol blue as indicator (both from Merck). The detection limit was determined to be 0.0015 M. The evaluation of the TVC was based on three column experiments for each resin. The relative standard deviation of the TVC values was determined to be about 2.9%.

The cleaning procedure of the resins was optimized to minimize organic leachables from the AERs in the batch and column experiments. The method is reported in Pürschel et al. [20]. In brief: washing with Millipore water (conductivity < 1 μS/cm, pH = 5.8 and TOC < 50 μg/L), threefold shaking (1 h) with 0.1 N NaOH (500 mL for 100 mL resin), treatment in a soxhlet reactor first with methanol, second with acetonitril (each for 24 h), washing with Millipore water and rinsing with 1 N NaOH (400 mL for 100 mL resin), 1.4 N HCl (300 mL for 100 mL resin) and again twice with

Table 1
Properties of the selected macroporous AERs

	Resin type			
	Weak and medium base AERs		Strong base AERs	
Parameters	IRA96[a]	AP246[b]	IRA900[a]	A860[c]
Functional group	Tertiary amine	Tertiary/quaternary amine, type I	Quaternary amine, type I	Quaternary amine, type I
Matrix material	Polystyrene	Polyacrylic	Polystyrene	Polyacrylic
Water content (%)	57–63	60–65	58–64	66–72
TVC—pH 6 (mol eq/L)	0.10 ± 0.01	0.39 ± 0.01	0.62 ± 0.02	0.63 ± 0.07
ρ_B (g/L)	670	710	700	700
ε_B (−)	0.362	0.343	0.343	0.352
d_P (mm)	0.73	0.47	0.735	0.725
r_P (mm)	0.365	0.235	0.3675	0.3625

Note: AERs = anion exchange resins; NOM = natural organic matter; TVC = total volume (anion exchange) capacity (median value ± measurement uncertainty after student *t*-distribution); ρ_B = bed density; ε_B = bed porosity; d_P = particle diameter; r_P = particle radius.

[a] Rohm and Haas, France S.A.S., Chauny Cedex, France.

[b] Bayer AG, Leverkusen, Germany.

[c] Purolite, Bala Cynwyd, USA.

1 N NaOH (each step with 4 BV/h) and final washing with Millipore water. All AERs were stored in Millipore water.

Several methods were compared to find the best way to dose accurately small quantities of resin without loss of TVC as a consequence of drying processes. It was found that preparation methods for anion exchangers from other authors, like vacuum filtration and storing in a desiccator for 24 h [21] or desiccation in vacuum at 325 K for 24 h [22], could not be applied for the AERs without a significant loss of TVC. Therefore, the Millipore water, in which the AERs were stored, was merely decanted before the resins were weighted. It was estimated by three parallel measurements for each AER that 1.00 ± 0.02 g wet resin is equal to 1.11 ± 0.05 mL resin volume, which is herein after referred to as reactor volume V_R.

3.2. Test water

The water used in the experiments was obtained from a water treatment plant in Boxberg, Germany (Vattenfall Europe Generation AG). The raw water, a mixture from the rivers Schwarze Schöps and Spree, was treated by coagulation ($Al_2(SO_4)_3$ and coagulant aid on polyacrylamide basis), neutralization/precipitation ($Ca(OH)_2$) and filtration (multi-layer filter containing anthracite and silica sand). This pre-treatment procedure is able to reduce the DOC concentration significantly depending on the NOM content and composition of the raw water [23,24]. The test water was collected after passing the pre-treatment and was kept at 5°C to prevent bacterial growth until use in experiments. The DOC, the composition of the NOM fractions as well as pH, conductivity, ion and SiO_2 concentrations of the test water are given in Table 2. Analytical methods are described in the next section (section 3.3).

The relatively high DOC concentration of the pre-treated water (4.08 mg/L) emphasizes the need of an enhanced NOM removal.

The pH of the water after pre-treatment was neutral (pH ≈ 7). Under neutral pH condition, NOM has a medium charge density due to the partial deprotonation of their acidic functional groups [7]. Thus, NOM uptake could occur by anion exchange, mainly onto strong base AERs with their quaternary amines, as well as by ion dipole and/or van der Waals interaction onto all AERs [4]. Further, hydrophobic NOM components could be adsorbed by π–π stacking and/or hydrophobic interactions onto the hydrophobic matrix of the resin, primarily onto polystyrene material [8,25]. Additionally, high sulphate and hydrogen carbonate concentrations were estimated in the test water. These ions could compete with weaker adsorbable NOM for polar anion exchange sites and therefore limit the NOM removal [26].

Table 2
Characterization of pre-treated water

Parameters	Values
DOC (μg/L)	4,083
HOC (μg/L)	465
Biopolymers (μg/L)	49
Humic substances (μg/L)	2,231
Building blocks (μg/L)	872
LMW neutrals (μg/L)	458
LMW acids (μg/L)	9
pH (–)	7.01
Conductivity (μS/cm)	570
Ca^{2+} (mg/L)	83.8
Mg^{2+} (mg/L)	14.0
Na^+ (mg/L)	19.1
K^+ (mg/L)	6.55
Cl^- (mg/L)	29.6
NO_3^- (mg/L)	15.9
SO_4^{2-} (mg/L)	167
HCO_3^- (mg/L)	274.50
SiO_2 (mg/L)	9.85

Note: DOC = dissolved organic carbon; HOC = hydrophobic organic carbon; LMW = low molecular weight.

3.3. Analyses

NOM was measured as DOC using a TOC analyser multi-N/C UV HS (Analytik Jena AG), based on wet chemical oxidation with an oxidation agent (sodium peroxodisulphate) and ultraviolet irradiation with subsequent infrared detection of the formed CO_2. Each sample was measured twice. The two-sample standard deviation was about 1.4%.

Advanced NOM characterization was carried out using LC–OCD following the method of Huber et al. [27]. The analyser was equipped with a chromatographic column (250 × 20 mm, TSK HW 50S, 3000 theoretical plates, Toso), which allows the separation of DOC into fractions depending on their molecular size (biopolymers, humic substances, building blocks, LMW neutrals and LMW acids). Prior to chromatographic separation, samples were filtered (0.45 μm PES filter, Sartorius). The fraction that remained on the chromatography column is calculated from the material balance and assigned to hydrophobic organic carbon (HOC). Organic carbon detection (OCD) was performed in a thin-film reactor with subsequent infrared detection. OCD calibration was based on potassium hydrogen phthalate. LC–OCD measurement of the test water sample was carried out by DOC Labour Dr Huber (Karlsruhe, Germany).

The pH was measured by a pH meter WTW pH 340 using a Sentix 41electrode, the conductivity by a conductivity meter WTW cond. 340 using a TetraCon 325electrode. Ion and SiO_2 analyses were performed in the analytical laboratory of the water treatment plant in Boxberg. Cation concentrations (Ca^{2+}, Mg^{2+}, Na^+ and K^+) were determined by inductively coupled plasma—optical emission spectrometry analysis (Optima 3300 DV, Perkin–Elmer), whereas anion concentrations (Cl^-, NO_3^-, SO_4^{2-}) were measured by ion chromatography analysis (Dionex ICS-1100, Thermo Scientific). The SiO_2 content in the water sample was investigated by photometric measurement (Lasa 100, Dr Lange).

3.4. Breakthrough curve measurement

The fixed-bed adsorption experiment was carried out in a glass column with an inside diameter of 1.0 cm. The column was filled with 5 mL of freshly regenerated and rinsed AER IRA96. Test water after pre-treatment (pH 7) was fed to the top of the column at a constant flow rate of 75 mL/h (equal to 0.96 m/h) regulated by a constant-speed tubing pump (IPC, Ismatec). The effluent samples were collected once per hour and NOM was measured as DOC. The overall error of a single concentration point in the BTCs was about 9.9%.

3.5. Parameter estimation for BTC modelling

In the present study, the software LDF 2.9 (© E. Worch, 2009) was applied for BTC modelling. The software is based on the LDF model and allows to consider competitive adsorption. For BTC modelling, equilibrium data as well as kinetic parameters of the NOM fractions are required. To characterize the NOM system, the fictive component approach (adsorption analysis) after Sontheimer et al. [16] and Johannsen and Worch [11] was used (see section 2.3). As a result of the adsorption analysis, the concentrations of the different NOM fractions (characterized by different Freundlich parameters) are obtained.

The DOC adsorption equilibrium data required for the adsorption analysis were received from batch experiments with constant solution volume (1.0 L) and varying AER resin volume and mass, respectively (V_R of 11, 27.5, 55, 110, 220, 330, 440 and 550 mL related to m_A of about 8, 19, 38, 76, 153, 229, 306, 382 mg). The flasks were shaken at room temperature with 200 rpm for 7 d, which proved in preliminary kinetic studies to be a sufficient time. After this contact time, the samples were decanted to separate the NOM solutions from the AERs. Next, concentration of NOM was measured as DOC. To validate the results, equilibrium experiments have been carried out twice. The two-sample standard deviation of one measurement was about 2.0%.

For the adsorption analysis, the Freundlich parameter n was set to be 0.5 for all adsorbable NOM fractions, whereas the K_F values were defined to be 0 $(mg/g)/(mg/L)^n$ for the non-adsorbable NOM fraction and 5, 20 and 80 $(mg/g)/(mg/L)^n$ for the weakly, moderately and strongly adsorbable NOM fractions, respectively. A search routine in the software AdsAna 1.4 (© E. Worch 2009) based on the IAST was used to find the concentration distribution of the NOM fractions which allows the best fitting of the experimental DOC equilibrium isotherm data.

Film and intraparticle mass transfer coefficients ($k_F a_{VR}$ and k_S^*, respectively) for the NOM fractions were obtained by the empirical correlations given in Eqs. (9)–(14). The $k_F a_{VR}$ values were calculated with a linear filter velocity of 0.95 m/h (equal to 75 mL/h) and a medium NOM molecular mass of 1,000 g/mol. For all adsorbable fractions, the same $k_F a_{VR}$ and k_S^* values were used.

4. Results and discussion

The experimental and calculated equilibrium data for NOM uptake (measured as DOC) from the pre-treated water onto four different macroporous AERs at neutral pH are shown in Fig. 1.

Table 3 summarizes the related concentration distributions found from the adsorption analysis of the different AERs.

As can be seen in Fig. 1, the definition of four fictive NOM fractions with the Freundlich parameters given in Table 3 allows describing the DOC isotherms in satisfactory quality for all studied AERs. Furthermore, the calculated initial concentrations of the different NOM fractions ($c_{0,i}$) vary between the different AERs.

The NOM adsorption behaviour characterized by the adsorption analysis can be taken as a quality measure in respect of the strength of the adsorption. The more the fictive component concentration distribution is shifted to the stronger adsorbable NOM fraction, the better NOM is adsorbed on the AER.

For all AERs, a relatively high fraction of non-adsorbable NOM was found (about 50%). The absolute concentrations of the non-adsorbable fraction differ

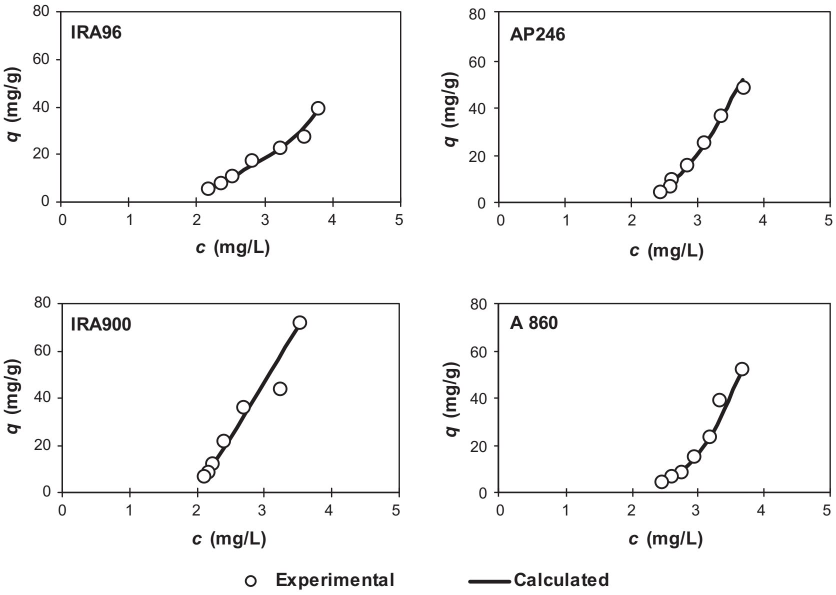

Fig. 1. Experimental equilibrium data and calculated adsorption analysis results for NOM uptake (measured as DOC) from pre-treated water onto four different macroporous AERs ($c_0 = 4.08$ mg/L DOC, pH 7).

Table 3
Adsorption analysis results of NOM uptake from pre-treated water onto four macroporous AERs ($c_0 = 4.08$ mg/L DOC, pH 7)

				Resin type			
				Weak and medium base AERs		Strong base AERs	
				IRA96	AP246	IRA900	A860
NOM fraction	Adsorption behaviour	K_F ((mg/g)/(mg/L)^n)	n (−)	$c_{0,i}$ (mg/L DOC)			
1	Non-adsorbable	0	–	1.94	2.33	2.02	2.27
2	Weakly adsorbable	5	0.5	0.54	0.29	0.11	0.59
3	Moderately adsorbable	20	0.5	1.22	0.71	0.67	0.45
4	Strongly adsorbable	80	0.5	0.37	0.75	1.28	0.76

Note: $c_{0,i}$ = calculated initial concentration of the NOM fraction i; mean percentage errors: 1.31% (IRA96), 1.29% (AP246), 2.49% (IRA900) and 0.98% (A860).

only slightly. A slightly lower amount of the non-adsorbable NOM fraction was found for polystyrene resins IRA96 and IRA900 ($c_{0,1} = 1.94$ and 2.02 mg/L DOC) than for polyacrylic resins AP246 and A860 ($c_{0,1} = 2.33$ and 2.27 mg/L DOC).

In the case of polyacrylic medium and strong base AERs AP246 and A860, the concentrations of the strongly adsorbed fraction are approximately the same ($c_{0,4} = 0.75$ and 0.76 mg/L DOC), whereas for AP246 a higher concentration of the moderately adsorbed fraction was found ($c_{0,3} = 0.71$ vs. 0.45 mg/L DOC). Consequently, AP246 shows a slightly better NOM uptake than A860.

In the case of polystyrene weak base AER IRA96, a larger fraction of NOM is moderately adsorbed ($c_{0,3} = 1.22$ mg/L DOC), but only a small amount of NOM is strongly adsorbed ($c_{0,4} = 0.37$ mg/L DOC). In contrast, the polystyrene strong base AER IRA900 shows the best adsorption performances because most of the adsorbable NOM is strongly adsorbed ($c_{0,4} = 1.28$ mg/L DOC) and the concentration of the weakly adsorbed NOM is very small ($c_{0,2} = 0.11$ mg/L DOC).

These results prove that under neutral conditions the medium and strong base resins AP246, IRA900 and A860 have higher overall NOM capacities and that a higher amount of NOM is strongly adsorbed in comparison to the weak base resin IRA96. This could be explained by the quaternary amines of the medium and strong base AERs, which act as anion acceptors enabling strongly polar/ionic interactions with hydrophilic organics, whereas the tertiary amines of the weak base AER are in uncharged form and less polar/ionic interactions occur. This outcome is in accordance with results from earlier studies (e.g. [2,4,7,28,29]), in which polar/ionic interactions between quaternary amine functional groups and NOM adsorbates were also proposed as the most important uptake mechanism under neutral pH conditions.

The differences between IRA900 on the one-hand side and AP246 and A860 on the other side could be explained by the different polymer composition of the AERs and the possibility of further interactions with specific NOM components. It can be assumed that humic substances, building blocks and LMW acids are preferentially removed by polar/ionic interaction between NOM acids/acidic components and the quaternary amines of the medium and strong base resins. In contrast, the NOM fractions of HOC, biopolymers and LMW neutrals could be primarily removed by physical adsorption (π–π stacking and/or hydrophobic interactions). As a consequence, the more hydrophobic polystyrene AERs are able to remove a higher amount of the HOC and hydrophobic neutrals fractions by physical adsorption than the polyacrylic resins [30,31]. In contrast, AERs with polyacrylic structure tend to be more hydrophilic and they have a more open structure and higher water content [7]. Thus, they exhibit enforced removal of larger molecules, like biopolymers, than the polystyrene ones [7,29].

In the present study, the fraction of hydrophobic/neutral organic compounds in the pre-treated water was significantly higher than the fraction of larger molecules like biopolymers (see Table 2). Consequently, the polystyrene strong base AER IRA900 with its more hydrophobic character is more efficient in overall NOM removal than the polyacrylic medium and strong base AERs AP246 and A860 with their more hydrophilic character.

As a result, it can be concluded that the combination of polystyrene matrix and quaternary amino groups provides the best condition for a high overall removal of different NOM fractions.

Additionally to the adsorption analysis results, kinetic parameters are needed for BTC modelling. For the NOM uptake from pre-treated water on four different AERs, the volumetric film and intraparticle (solid) mass transfer coefficients ($k_F a_{VR}$ and k_S^*) were calculated by empirical correlations after Wilson and Geankoplis [17] and Hess [19] for $M = 1{,}000$ g/mol, $v_F = 0.96$ m/h and $c_0 = 4.08$ mg/L DOC. Both estimated mass transfer coefficients are given in Table 4.

The $k_F a_{VR}$ and k_S^* values for NOM adsorption at neutral pH were found to be in the range 0.05–0.12 s^{-1} and 3.4–4.0×10^{-6} s^{-1}, respectively.

Fig. 2 depicts the modelled BTCs for the NOM uptake from pre-treated water onto IRA96, AP246, IRA900 and A860 together with the experimental BTC for IRA96.

For AER IRA96, it could be proved that the prediction of the NOM breakthrough by the LDF model on the basis of an adsorption analysis is successful (see Fig. 2). Obviously, the applied BTC model as well as the fictive component approach, both originally developed for activated carbon adsorption, can also be applied to NOM uptake on AERs. Moreover, the empirical correlation for estimating the intraparticle (solid) diffusion coefficient of NOM can also be extended to NOM adsorption on AERs.

The predicted breakthrough behaviour reflects the results of the adsorption analysis. For all AERs, an instantaneous breakthrough is predicted, according to the existence of a non-adsorbable fraction. The polystyrene weak base AER IRA96, for which a very low amount of NOM was characterized by the adsorption analysis as strongly adsorbable, shows the fastest breakthrough (90% after a throughput of 15,000 BV). In contrast, in the polystyrene strong base AER IRA900 where the highest fraction of NOM is strongly adsorbed, the breakthrough concentrations increase much slower (70% breakthrough after 15,000 BV). The BTCs of the polyacrylic weak and medium base AERs AP246 and A860 did not differ very much; they are located between those of IRA96 and IRA900.

In sum, at neutral pH conditions, the polystyrene strong base AER IRA900 removed the highest amount of the strongly adsorbable NOM fraction and shows the highest overall NOM capacity.

Table 4
$k_F a_{VR}$ and k_S^* values for NOM uptake from pre-treated water (pH 7) onto four macroporous AERs ($M = 1{,}000$ g/mol, $v_F = 0.96$ m/h, $c_0 = 4.08$ mg/L DOC)

	Resin type			
	Weak and medium base AERs		Strong base AERs, type I	
Parameters	IRA96	AP246	IRA900	A860
$k_F a_{VR}$ (s^{-1})	0.5×10^{-1}	1.2×10^{-1}	0.6×10^{-1}	0.6×10^{-1}
k_S^* (s^{-1})	3.5×10^{-6}	4.0×10^{-6}	3.5×10^{-6}	3.4×10^{-6}

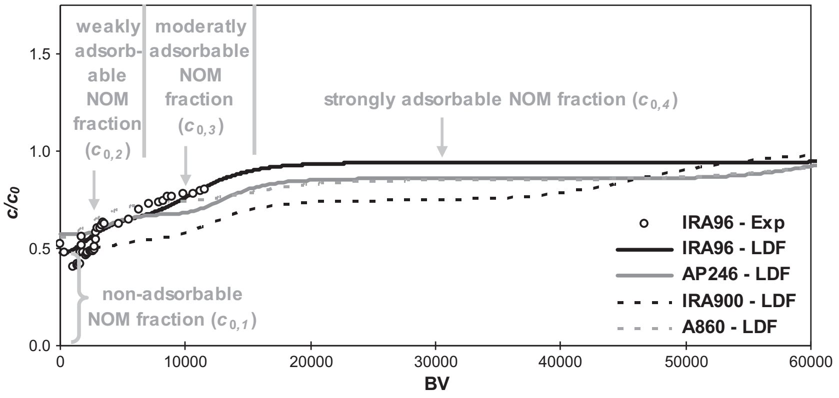

Fig. 2. BTCs for NOM concentrations (measured as DOC) from pre-treated water onto four AERs (experimentally (Exp) determined and/or calculated by the LDF model with NOM fractions obtained by adsorption analysis; BV = input solution volume related to reactor volume; $c_0 = 4.08$ mg/L DOC, pH 7).

5. Conclusions

- In the present work, the adsorption behaviour of NOM on different AERs was studied at neutral pH. The DOC isotherms could be described successfully by the adsorption analysis based on the assumption of four NOM fractions with different adsorption strengths.
- The results of the adsorption analysis (concentrations and Freundlich parameters of the fictive components) together with empirically estimated film and intraparticle (solid) mass transfer coefficients could be used to predict BTCs of the NOM adsorption onto different AERs by the LDF model for competitive adsorption.
- The applicability of the BTC prediction model was verified with the experimentally determined BTC for NOM uptake onto AER IRA96. It could be shown that the modelling approach (adsorption analysis in combination with the LDF model), originally developed for activated carbon adsorption, can be also used as tool to evaluate and predict the NOM uptake in AER fixed-bed filters.
- For the studied pre-treated water, higher overall NOM uptake capacities at neutral pH were found for medium and strong base AERs AP246, IRA900 and A860 than for the weak base AER IRA96. This could be explained by the positively charged quaternary amines of the medium and strong base AERs that allow polar/ionic interactions with the hydrophilic NOM fractions, whereas the tertiary amines of the weak AER are mainly in uncharged form and should be less able to perform polar/ionic interactions under neutral pH conditions. For strong base AERs, an enforced NOM capacity was estimated for the polystyrene resin IRA900 than for the polyacrylic resin A860, most probably due to an improved uptake of hydrophobic/neutral NOM components onto the polystyrene matrix by π–π stacking and/or hydrophobic interactions and low impact of size exclusion limitation due to NOM composition in the pre-treated water sample.
- In view of these results, the application of polystyrene strong base AERs is an option to remove specific NOM fractions, especially the HOC, low to medium molecular size biopolymers as well as the LMW neutrals, from water in drinking water treatment plants.
- In future studies, regeneration experiments should be carried out for all AERs to study their specific fouling character.

List of symbols

a — empirical parameter (s^{-1})
a_{VR} — volume-related surface area (m^{-1})
b — empirical parameter (m^2 L)/(mg s)
c — concentration in the fluid phase (mg/L)
c_s — concentration at the outer solid particle surface (mg/L)
c_0 — inlet concentration (mg/L)
$c_{0,a}$ — total concentration of all adsorbable NOM fractions (mg/L)
D_L — liquid film diffusion coefficient (m^2/s)
d_P — particle diameter (m)
K_F — parameter of the Freundlich isotherm (mg/g)/(mg/L)^n
k_F — film mass transfer (m/s)
$k_F a_{VR}$ — volumetric film mass transfer coefficient (s^{-1})
k_S — mass transfer coefficient (m/s)

k_S^* — intraparticle mass transfer coefficient (s^{-1})
M — molecular mass of the solute (g/mol)
m_A — adsorbent mass (g)
n — exponent of the Freundlich isotherm (–)
q — equilibrium adsorbent loading corresponding to c (mg/g)
q_s — adsorbent loading at the outer particle surface (mg/g)
q_T — total amount adsorbed (mg/g)
$\bar{q}$ — mean adsorbent loading of the solid phase (mg/g)
Re — Reynolds number (–)
r_P — particle radius (m)
Sc — Schmidt number (–)
Sh — Sherwood number (–)
T — temperature (K)
t — time (s)
V_L — volume of the liquid phase (L)
V_R — reactor volume (L)
v_F — linear filter velocity (m/s)
z — vertical travel distance within the adsorber (m)
z_i — adsorbed phase mol fraction (–)
ε_B — bed porosity (–)
η — dynamic viscosity (Pa•s)
ρ_B — bed density (g/L)
v — kinematic viscosity (m^2/s)
φ — spreading pressure term (–)

Acknowledgements

The authors thank Dr Torsten Lehmann for his helpful support in water sampling and analysis in the power plant Boxberg, and stud. chem. Thomas Petrick for his extensive experimental labwork. We are grateful to Vattenfall PowerConsult GmbH and Vattenfall Europe Generation AG for financial support of this work. Further, we thank Rohm and Haas France S.A.S., Bayer AG and Purolite for providing us with the anion exchange resins.

References

[1] R.F. Christman, M. Ghassemi, Chemical nature of organic color in water, J. Am. Water Works Assoc. 58 (1996) 723.

[2] J.-P. Croue, D. Violleau, C. Bodaire, B. Legube, Removal of hydrophobic and hydrophilic constituents by anion exchange resin, Water Sci. Technol. 40 (1999) 207–214.

[3] D. Van der Kooij, Biological stability: A multidimensional quality aspect of treated water, Water Air Soil Poll. 123 (2000) 25–34.

[4] B. Bolto, D. Dixon, R. Eldridge, S. King, K. Linge, Removal of natural organic matter by ion exchange, Water Res. 36 (2002) 5057–5065.

[5] J. Fettig, Modelling the uptake of natural organic matter (NOM) by different granular sorbent media, J. Water Supply Res. Technol.—AQUA 54 (2005) 83–93.

[6] A. Genz, B. Baumgarten, M. Goernitz, M. Jekel, NOM removal by adsorption onto granular ferric hydroxide: Equilibrium, kinetics, filter and regeneration studies, Water Res. 42 (2008) 238–248.

[7] T.H. Boyer, P.C. Singer, Stoichiometry of removal of natural organic matter by ion exchange, Environ. Sci. Technol. 42 (2008) 608–613.

[8] E.R. Cornelissen, N. Moreau, W.G. Siegers, A.J. Abrahamse, L.C. Rietveld, A. Grefte, M. Dignum, G. Amy, L.P. Wessels, Selection of anionic exchange resins for removal of natural organic matter (NOM) fractions, Water Res. 42 (2008) 413–423.

[9] S.G.J. Heijman, A.M. Van Paassen, W.G.J. van der Meer, R. Hopman, Adsorptive removal of natural organic matter during drinking water treatment, Water Sci. Technol. 40 (1999) 183–190.

[10] Y. Tan, J.E. Kilduff, Factors affecting selectivity during dissolved organic matter removal by anion-exchange resins, Water Res. 41 (2007) 4211–4221.

[11] K. Johannsen, E. Worch, Eine mathematische Methode zur Durchführung von Adsorptionsanalysen (A mathematical method for evaluation of adsorption analysis), Acta Hydroch. Hydrob. 22 (1994) 225–230.

[12] E. Glueckauf, Theory of chromatography, Part 10, Formula for diffusion into spheres and their application to chromatography, Trans. Faraday Soc. 51 (1955) 1540–1551.

[13] E. Worch, Adsorption Technology in Water Treatment. Fundamentals Processes and Modeling, De Gruyter, Berlin, 2012.

[14] E. Worch, Zur Vorausberechnung der Gemischadsorption in Festbettadsorbern Teil 1: Mathematisches Modell (Prediction of mixture adsorption in fixed-bed adsorbers. Pt. 1: Mathematical model), Chem. Tech. 43 (1991) 111–113.

[15] E. Worch, Zur Vorausberechnung der Gemischadsorption in Festbettadsorbern Teil 2. Anwendung des Berechnungsmodells auf experimentell untersuchte Systeme (Prediction of mixture adsorption in fixed bed adsorbers. Pt. 2: Application of the calculation model to experimentally investigated systems), Chem. Tech. 43 (1991) 221–224.

[16] H. Sontheimer, J.C. Crittenden, R.S. Summers, Activated Carbon for Water Treatment, DVGW Forschungsstelle, Karlsruhe, 1988.

[17] E.J. Wilson, C.J. Geankoplis, Liquid mass transfer at very low Reynolds numbers in packed beds, Ind. Eng. Chem. Fundam. 5 (1966) 9–14.

[18] E. Worch, Eine neue Gleichung zur Berechnung von Diffusionskoeffizienten gelöster Stoffe (A new equation for the calculation of diffusion coefficients for dissolved substances), Vom Wasser 81 (1993) 289–297.

[19] F. Hess, Entwicklung praxisorientierter Berechnungsgrundlagen für die Kinetik der Aktivkohlefiltration in der Trinkwasseraufbereitung (Development of practice-oriented design fundamentals for activated carbon filtration in drinking water treatment), PhD thesis, Dresden University of Technology, Dresden, 2001.

[20] M. Pürschel, E. Worch, V. Ender, Uptake of NOM fractions by anion-exchange resins in demineralization plants, Desalin. Water Treat. (2013), doi: 10.1080/19443994.2013.825884 (accessed August 01, 2013).

[21] T.H. Boyer, P.C. Singer, G.R. Aiken, Removal of dissolved organic matter by anion exchange: Effect of dissolved organic matter properties, Environ. Sci. Technol. 42 (2008) 7431–7437.

[22] W. Zhang, C. Hong, B. Pan, Q. Zhang, P. Jiang, K. Jia, Sorption enhancement of 1-naphthol onto a hydrophilic hyper-cross-linked polymer resin, J. Hazard. Mater. 163 (2009) 53–57.

[23] S.A. Huber, The behaviour of natural organic matter in water treatment and the water water/steam cycle: Deeper insights, Power Plant Chem. 8 (2006) 105–116.

[24] P. Hübner, Organics removal in water treatment plants, Power Plant Chem. 13 (2011) 426–435.

[25] P. Li, A.K. Sengupta, Sorption of hydrophobic ionizable organic compounds (HIOCs) onto polymeric ion exchangers, React. Funct. Polym. 60 (2004) 27–39.

[26] C.T. Anderson, W.J. Maier, Trace organics removal by anion exchange resins, J. Am. Water Works Assoc. 71 (1979) 278–283.

[27] S.A. Huber, A. Balz, M. Abert, W. Pronk, Characterisation of aquatic humic and non-humic matter with size-exclusion chromatography—organic carbon detection—organic nitrogen detection (LC-OCD-OND), Water Res. (2011) 879–885.

[28] Y. Tan, J.E. Kilduff, M. Kitis, T. Karanfil, Dissolved organic matter removal and disinfection byproduct formation control using ion exchange, Desalination 176 (2005) 189–200.

[29] M. Pürschel, S. Sachs, G. Bernhard, V. Ender, Uptake of multi-disperse starch by anion exchangers, J. Phys. Sci. Appl. 3 (2013) 147–155.

[30] M. Gottlieb, The reversible removal of naturally occurring organics using resins regenerated with sodium chloride, Ultrapure Water 11 (1996) 53–58.

[31] H. Humbert, H. Gallard, H. Suty, J.-P. Croué, Performance of selected anion exchange resins for the treatment of a high DOC content surface water, Water Res. 39 (2005) 1699–1708.